Applied Surface Science 404 (2017) 318–325

Contents lists available at ScienceDirect

Applied Surface Science

journal homepage: www.elsevier.com/locate/apsusc

Full Length Article

Thermochemical micro imprinting of single-crystal diamond surface using a nickel mold under high-pressure conditions

Yuji Imoto, Jiwang Yan*

Department of Mechanical Engineering, Faculty of Science and Technology, Keio University, Hiyoshi 3-14-1, Kohoku-ku, Yokohama 223-8522, Japan

ARTICLE INFO

Article history:
Received 13 November 2016
Received in revised form 5 January 2017
Accepted 30 January 2017
Available online 1 February 2017

Keywords:
Single-crystal diamond
Microstructure
Nickel mold
Imprinting
Thermochemical reaction
Carbon diffusion

ABSTRACT

Single-crystal diamond is an important material for cutting tools, micro electro mechanical systems, optical devices, and semiconductor substrates. However, the techniques for producing microstructures on diamond surface with high efficiency and accuracy have not been established. This paper proposes a thermochemical imprinting method for transferring microstructures from a nickel (Ni) mold onto single-crystal diamond surface. The Ni mold was micro-structured by a nanoindenter and then pressed against the diamond surface under high temperature and pressure in argon atmosphere. Results show that microstructures on the Ni mold were successfully transferred onto the diamond surface, and their depth increased with both pressure and temperature. Laser micro-Raman spectroscopy, transmission electron microscopy (TEM) and electron energy loss spectroscopy (EELS) analyses indicate that a graphite layer was formed over the contact area between diamond and Ni during pressing, and after washing by a mixed acid, the graphite layer could be completely removed. This study demonstrated the feasibility of a cost-efficient fabrication method for large-area microstructures on single-crystal diamond.

© 2017 Elsevier B.V. All rights reserved.

1. Introduction

Single-crystal diamond has the highest hardness, excellent thermal conductivity, optical property, electric insulation and chemical stability. It is now used as an ultraprecision cutting tool material, and is expected to be applied to semiconductor substrates, micro electro mechanical systems (MEMS), and optical devices in the future. For these applications, cost-efficient precision micromachining of single-crystal diamond is demanded. Currently, laser machining, focused ion beam (FIB) machining, and reactive ion etching (RIE) methods are used for fabricating microstructures on diamond [1–4]. However, these methods lead to very high processing cost and low productivity, which limits the applications of diamond.

Although diamond is extremely hard, and difficult to be mechanically processed, it might be thermochemically machined in an easier manner. It has been reported that the tool wear is very severe when cutting transition metals, such as Ni, Co, Ti, Fe, and so on, using a diamond tool [5–9]. A thermochemical reaction occurs between diamond and transition metals, where carbon atoms in diamond are diffused into the transition metals. In recent years, surface processing of diamond utilizing the aforementioned thermochemical reaction has gathered extensive attention [10–16]. For example, a patterned Ni layer was used to react with diamond to provide surface patterning in a large area [17] without necessity of using strict vacuum environment. However, it is time-consuming to perform Ni coating/patterning on diamond, and to remove the Ni coating after the thermochemical reaction.

In this study, we propose a novel thermochemical imprinting process for single-crystal diamond. A micro-structured Ni mold surface is pressed onto diamond surface under high temperature and pressure to transfer the microstructures from the Ni mold to the diamond workpiece through interfacial thermochemical reaction. The shape, depth, and distribution of the microstructures on the Ni mold are flexibly and precisely controlled by a nanoindentation system, and the thermochemical reaction between the mold and the diamond workpiece is controlled by pressure and temperature for various processing depth.

This paper presents experimental results of microstructure formation behavior on single-crystal diamond in the thermochemical imprinting process. The influence of pressure and temperature on the imprinting depth will be examined. The feasibility of cost-efficient fabrication of high-precision microstructures on single-crystal diamond by the proposed method will be demonstrated.

2. Process mechanism

Fig. 1 illustrates schematically the process mechanism for thermochemical imprinting. First, micro dimples are formed on a Ni

* Corresponding author.
E-mail address: yan@mech.keio.ac.jp (J. Yan).

http://dx.doi.org/10.1016/j.apsusc.2017.01.303
0169-4332/© 2017 Elsevier B.V. All rights reserved.

Downloaded from Yan Laboratory, Keio University at http://www.yan.mech.keio.ac.jp. Redistribution is subject to copyright licence from the journal publisher.

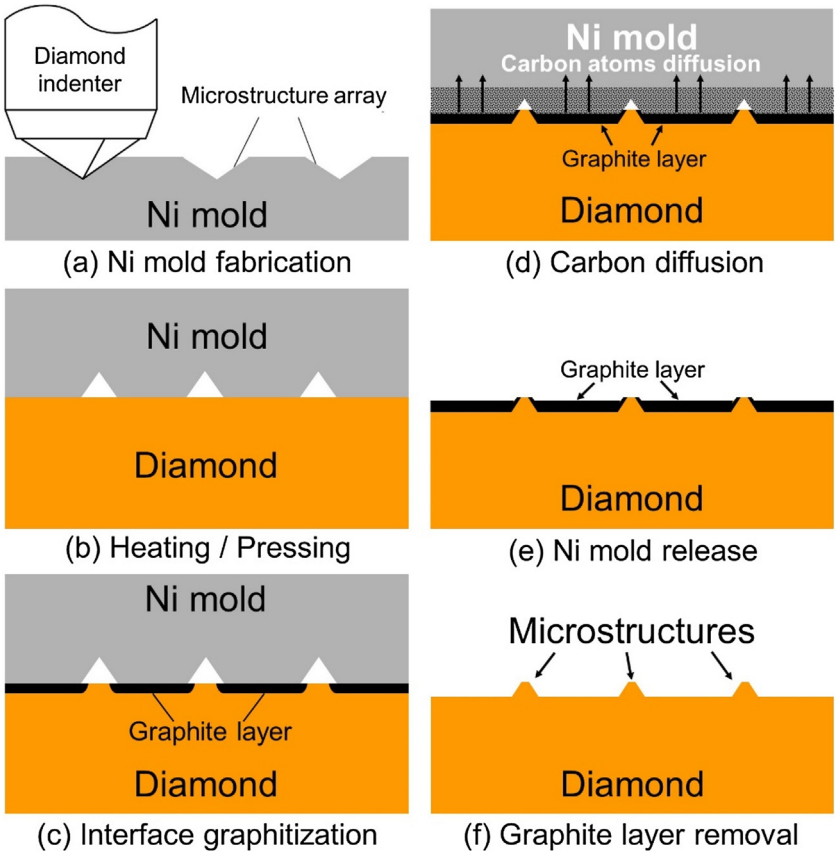

Fig. 1. Schematic diagram of micro imprinting process based on thermomechanical reaction.

mold surface by a diamond indenter (a). After the Ni mold gets into contact with a diamond substrate, they are pressed together and heated (b). At high temperature, the diamond surface will be easily wetted by nickel. Under the catalytic effect of nickel, diamond tends to undergo a phase transformation from diamond to graphite [18,19], and a thin layer of graphite is formed at the Ni-diamond interface (c). Subsequently, the graphitic carbon at the Ni-diamond interface will diffuse into the nickel mold (d). The rise of temperature reduces the energy barrier for graphitization and also improves the solubility of carbon in nickel. As a result of continuous graphitization and diffusion, the diamond surface is locally machined deeper and deeper. After this, the sample is cooled down and the Ni mold is removed from the diamond substrate by immersing the sample in hydrochloric acid HCl (e). Finally, the graphite layer is removed by a mixed acid, and microstructures are obtained on the diamond surface (f).

3. Experimental procedures

3.1. Materials

Single-crystal diamond square pieces with a dimension of 3.0 mm × 3.0 mm × 1.5 mm were used as specimen. The top planes of the diamond samples were (100). The diamond surfaces were then polished to a mirror finish by a cast iron scaif. The Ni mold material, provided by Nilaco Co., Japan, contains 99.6% Ni, 0.20% Mn, 0.07% Fe, 0.05% Si and 0.008% C by mass. The Ni molds were formed from a Ni rod to a dimension of ϕ6 mm × 2 mm by a wire electric discharge machine, Mitsubishi MV2400S (Mitsubishi Electric Co., Japan). The surface of the cut Ni pieces were polished to mirror surface by a polishing machine, EJW-400IFN-D (Engis Japan Co., Japan). Concentrated hydrochloric acid (HCl), nitric acid (HNO_3) and sulfuric acid (H_2SO_4) provided by Junsei Chemical Co., Ltd, Japan were used as solvents for washing the processed samples.

3.2. Micro-structuring of molds

A nanoindentation system, ENT-1100a (Elionix Inc., Japan), which was originally designed for evaluating material mechanical properties, was used to fabricate microstructures on the Ni molds. The indentation force and loading rate can be precisely controlled, enabling generation of micro dimples with various depths. Unlike a cutting process, the temperature increase of the diamond indenter is extremely small during nanoindentation, thus the thermochemical reaction between diamond and the Ni mold can be suppressed. Additionally, the shape of microstructure is decided by the shape of the diamond indenter. A photograph of an indented Ni mold is shown in Fig. 2(a), where the microstructures were formed in the mold center within an area of 1 mm × 1 mm. Fig. 2(b) and (c) show a conical dimple array and a pyramidal dimple array formed on the Ni mold. It should be noted that pileups might be generated around the dimples during indentation, especially when indenting deep dimples. However, in the subsequent press molding stage, the pileups can be pressed and flattened by the diamond surface, thus have little effect on the imprinting process.

3.3. Molding conditions

Fig. 3 illustrates the high-precision molding machine GMP211 (Toshiba Machine Co. Ltd., Japan) used in this study. The machine can control precisely the molding temperature and force in different atmospheric gases. Heating is realized by infrared lamps and temperature was monitored by a thermocouple with ±1 °C accuracy. The pressing force ranges from 0.2 kN to 20 kN with a res-

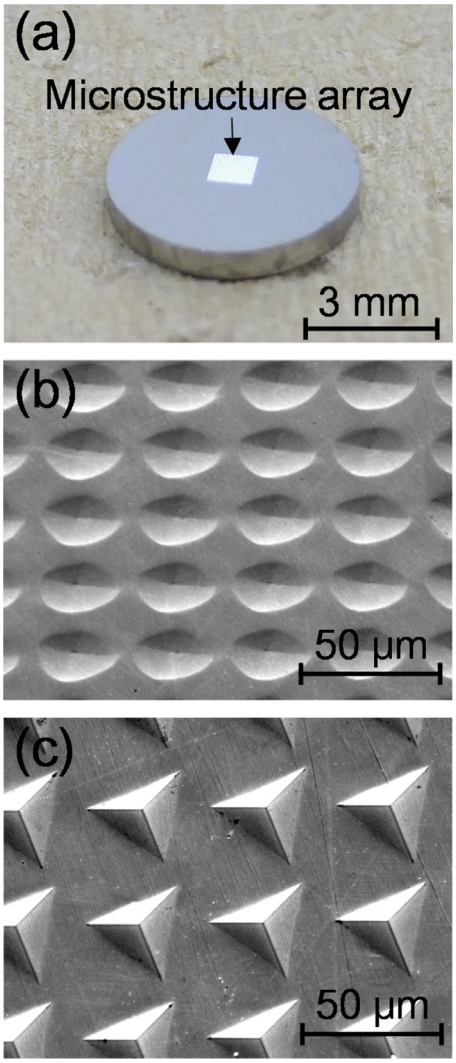

Fig. 2. (a) Photograph of a Ni mold; SEM images of microstructures formed on the Ni mold: (b) conical dimple array, (c) pyramidal dimple array.

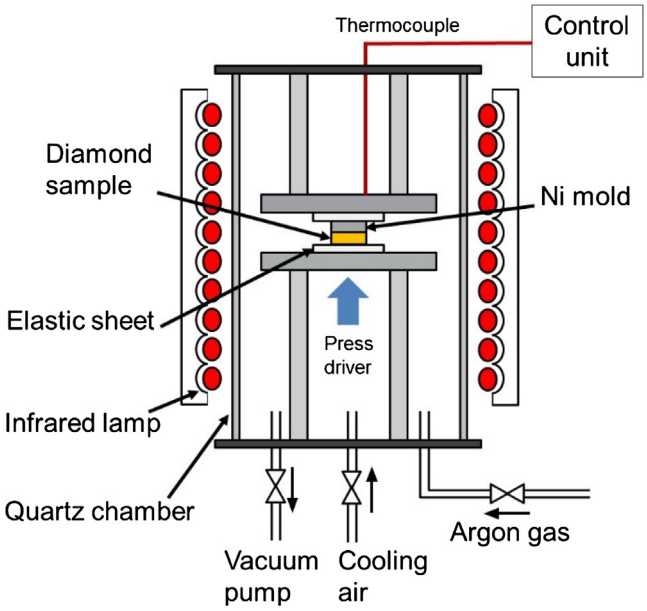

Fig. 3. Schematic diagram of the high-precision press molding machine.

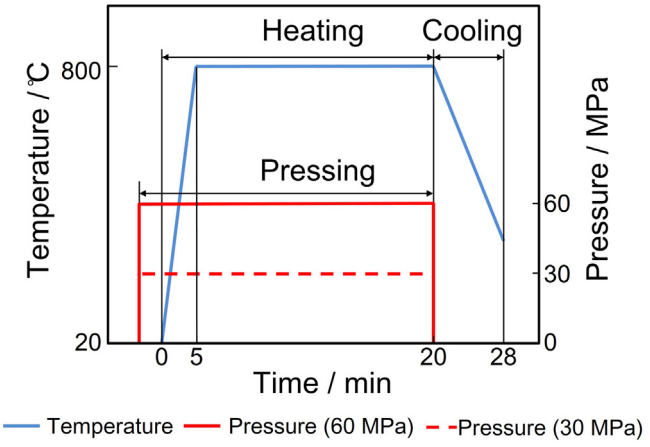

Fig. 4. Molding cycle of temperature and pressure used for thermochemical imprinting.

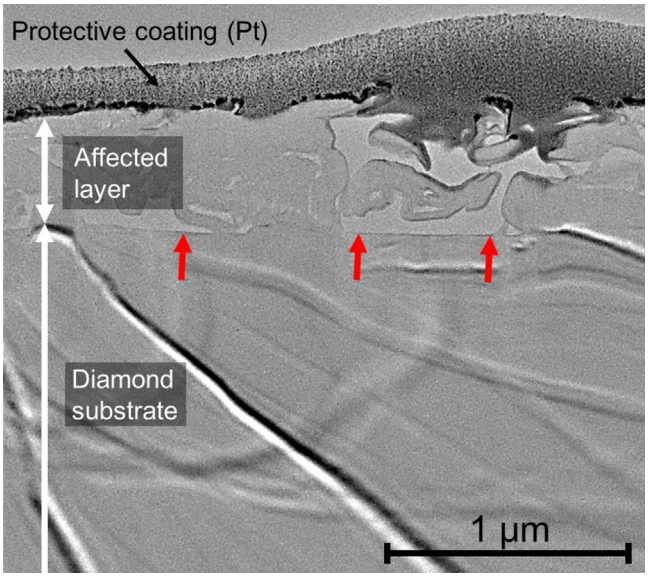

Fig. 5. Cross-sectional TEM image of a flat diamond sample after pressing.

olution of 0.98 N. The molding chamber is covered by a transparent quartz tube, in which an atmospheric gas (Ar or N_2) is purged. To prevent from uneven contact and force concentration between the diamond sample and the Ni mold, ceramic elastic sheets were used to cover the diamond sample and the Ni mold from two sides.

The thermal cycle and pressure change used in this study is shown in Fig. 4. Since carbon diffusion from diamond to transition metals is temperature dependent [6,18–20] and only occurs when temperature is above ~600 °C, in the present experiments, the heating temperature of the molds was set to 600 °C, 650 °C, 700 °C, 750 °C and 800 °C, respectively. The thermochemical reaction is also influenced by atmosphere gas [1]. The reaction efficiency is higher in a noble gas compared to in other gases [21]. In this study, argon (Ar) gas was used to purge the molding chamber.

The major steps of molding press are described as follows. (1) The diamond sample and the Ni mold are placed between two ceramic elastic sheets, and then compression starts until a preset molding pressure (~60 MPa) is reached. (2) Ar gas is purged into the quartz chamber for 20 s in order to increase the thermochemical reaction efficiency and prevent the oxidation of Ni mold. (3) The diamond sample and the Ni mold are rapidly heated by the infrared lamps from room temperature to the preset molding temperature (~800 °C) at a heating rate of 99 °C/min. (4) The temperature retains

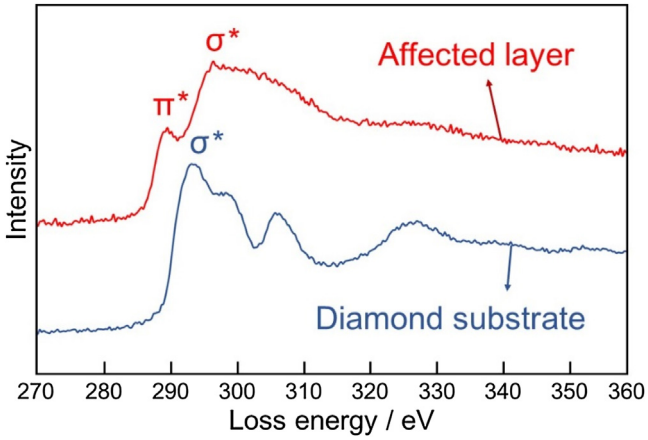

Fig. 6. EELS spectra of different regions of the sample cross section: diamond substrate and affected layer.

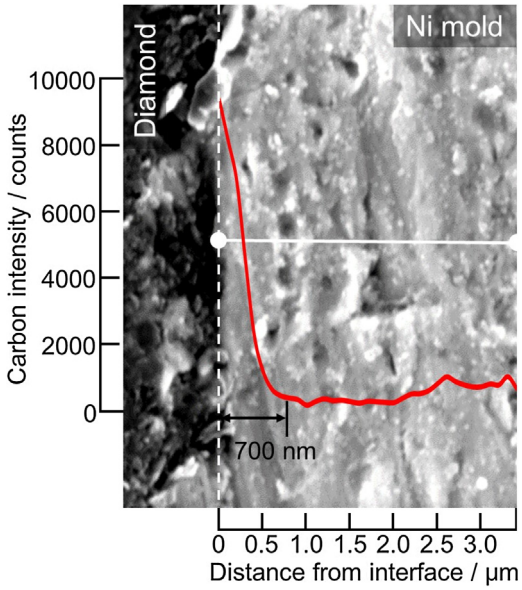

Fig. 7. EDS intensity profile of carbon in the Ni mold.

for 15 min. (5) The compression stops, and cooling starts at a rate of 99 °C/min by purging Ar gas into the chamber. (6) The Ni mold is removed from the diamond sample by HCl at 150 °C.

3.4. Surface/subsurface characterization

The microstructures formed on the diamond surface were observed using an environment scanning electron microscope (E-SEM) (Inspect S50, FEI Co., USA) and a field emission scanning electron microscope (FE-SEM) (Sirion, FEI Co., USA). Before SEM observation, the diamond specimen was coated with osmium in order to increase electrical conductivity. The elements of the sample surface were detected by an energy dispersive X-ray spectroscope (EDS) (XFlash Detector 4010, Bruker Co., Germany). The crystalline structure of the diamond surface was characterized by a laser micro-Raman spectroscope (NRS-3100, JASCO Co., Japan). The cross section of the thermochemical reacted surface was observed using a transmission electron microscope (TEM) (Tecnai G2, FEI Co., USA) with electron energy loss spectroscopy (EELS) function. The TEM sample was prepared by thinning the sample using a focused ion beam (FIB) equipment (Quanta3D FEG, FEI Co., USA). The microstructure height and the surface roughness were measured using a white-light interferometer (CCI3D, Taylor Hobson Co., Ltd, UK).

4. Results and discussion

4.1. Analysis of imprinted surface

Fig. 5 shows a cross-sectional TEM image of a flat diamond sample pressed at 30 MPa. From this result, it is clear that an affected layer (~500 nm deep) was formed after the thermochemical reaction (The boundary between the affected layer and the diamond substrate is indicated by three red arrows in the figure). For further analyzing the structure of the affected layer, EELS measurement

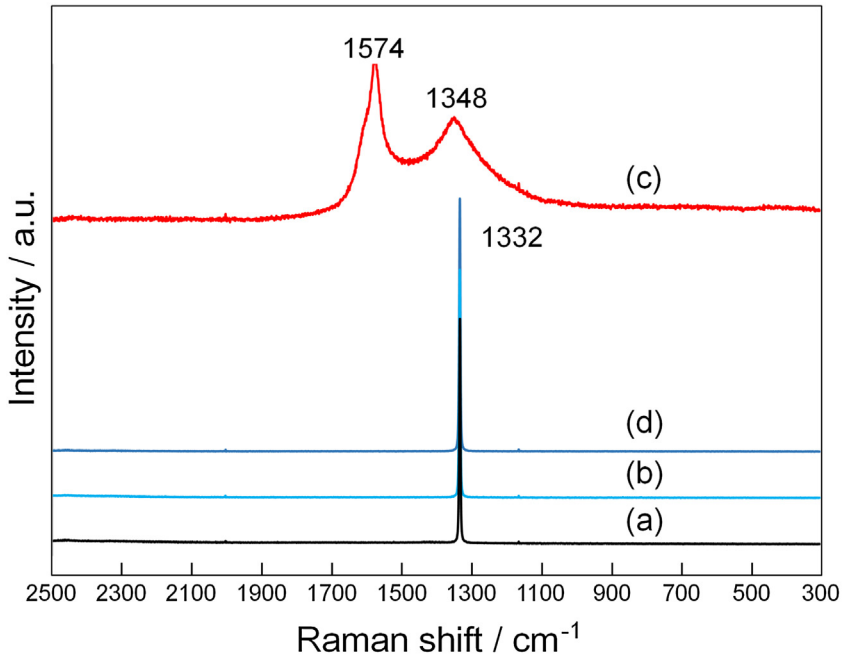

Fig. 8. Raman spectra of different diamond surfaces: (a) initial state, (b) non-reacted area, (c) reacted area, (d) after oxidative decomposition.

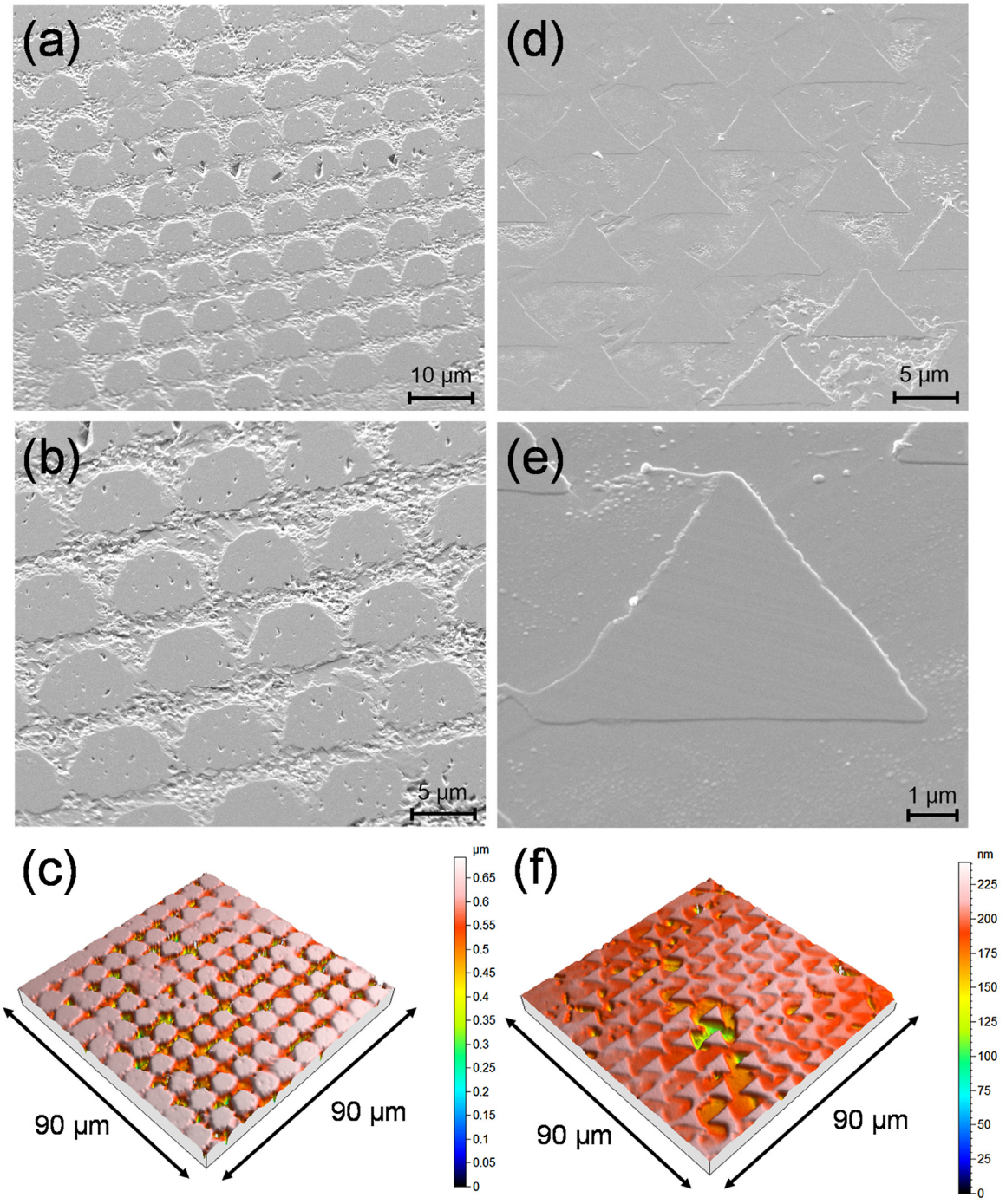

Fig. 9. SEM images and three-dimensional profiles of microstructures fabricated on diamond: (a)–(c) formed by a mold with conical dimples; (d)(f) formed by a mold with pyramidal dimples.

was done and the results are presented in Fig. 6. The EELS spectrum detected on the diamond substrate shows peaks at loss energy higher than 290 eV, indicating anti-bonding σ^* orbital of C—C bonding. This result means the substrate is composed of single-crystal diamond [22]. On the other hand, the EELS spectrum of the affect layer shows a peak from 280 eV to 290 eV indicating anti-bonding π^* orbital of C=C bonding, which means that the affected layer was transformed to graphite structure. The results in Figs. 5 and 6 indicate that a 500 nm thick graphite layer was generated on the diamond substrate during the thermochemical reaction with the Ni mold.

SEM/EDS analysis was conducted near the interface of the Ni mold and the diamond workpiece, and the result is shown in Fig. 7. Carbon was detected in the surface layer (~700 nm deep) of the Ni mold, and the carbon intensity detected near the interface with the diamond workpiece is distinctly higher than that of the inner region. This result strongly demonstrates that carbon atoms have been diffused into the Ni mold from the diamond surface during press molding. It is presumable that the carbon diffusion phenomenon is closely related to (or might be a reason for) the graphite layer formation on the diamond workpiece.

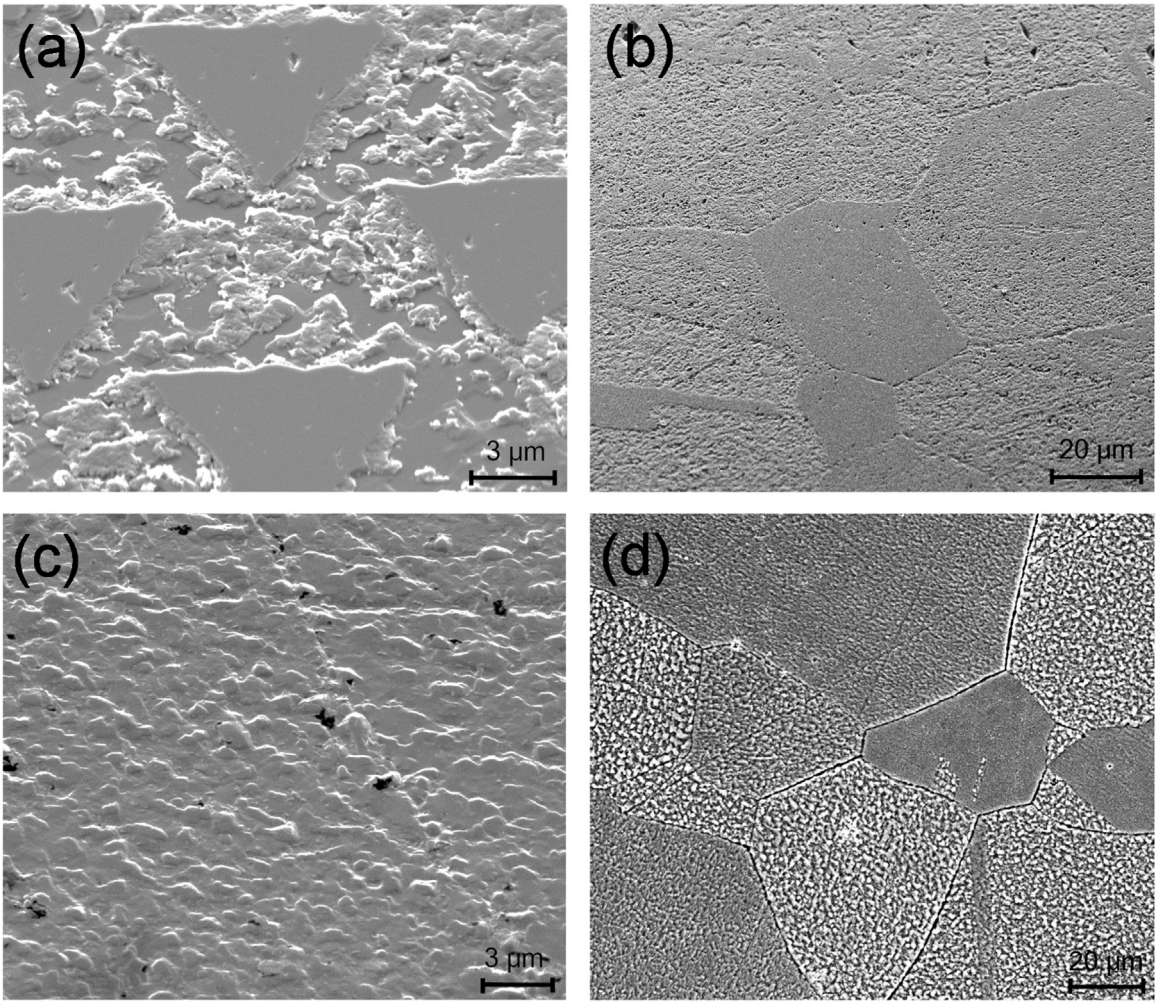

Fig. 10. SEM images of (a) rugged texture and (b) tessellated texture on diamond surface after pressing. (c) and (d) are Ni surfaces after heat treatment without pressing, showing similar surface textures to those in (a) and (b).

4.2. Removal of graphite layer

The graphite layer affects the properties of diamond, and should be removed after the imprinting process. For removing the graphite layer, oxidative decomposition treatment was conducted using a mixed acid (H_2SO_4:$HClO_4$: conc. HNO_3 = 5:3:1, in volume ratio) at 200 °C for 120 min [23,24]. To confirm the surface structure before/after the removal of the graphite layer, laser micro-Raman measurement was done, as shown in Fig. 8. For comparison, both the reacted area and the non-reacted area were measured. The Raman spectrum (a) detected on the initial diamond surface before the experiment shows a sharp peak at 1332 cm^{-1}. Similarly, the spectrum (b) measured on the non-reacted area also presents a peak at 1332 cm^{-1}, indicating the non-reacted diamond surface was not affected in the experiment. In the thermochemical reacted area, the spectra (c) shows peaks at 1348 cm^{-1} and 1574 cm^{-1}, indicating graphitization of diamond [25], which is in agreement with the TEM/EELS results in Fig. 6. In contrast, the Raman spectrum (d) obtained from the surface after oxidative decomposition treatment shows only a sharp peak at 1332 cm^{-1}, demonstrating that the graphite layer was successfully removed by the oxidative decomposition treatment. In Fig. 8, no peak was detected at around 400 cm^{-1} and 2400 cm^{-1}, indicating that the graphite layer has been formed without metal (Ni) bonding.

4.3. Microstructure formation

Fig. 9 shows SEM photographs and three-dimensional profiles of diamond surfaces after removal of the graphite layers. The molding temperature was 800 °C, and pressure was 30 MPa for these samples. In the figure, (a)–(c) are microstructures formed by a mold indented with conical dimples, while (d)–(f) are formed by another mold structured with pyramidal dimples. The microstructures indented on the Ni molds have been successfully transferred to the diamond surfaces, and the top surfaces of these microstructures are smooth.

At a molding temperature of 800 °C, the bottom surfaces of the microstructures, i.e., the surface areas contacting with Ni, are rough with rugged and tessellated textures, as shown in Fig. 10(a) and (b). In order to identify the reason for these rough surface textures, a heat treatment test was performed by only heating a Ni mold at 800 °C in Ar atmosphere for 15 min without molding press. Fig. 10(c) and (d) shows photographs of the Ni mold surface after the heat treatment. The rugged textures of the Ni mold after the heat treatment in Fig. 10(c) are very similar to that in Fig. 10(a), and the tessellated textures in Fig. 10(d) are similar to those in Fig. 10(b). This fact indicates that the Ni mold surface becomes rugged and tessellated during heating, and these surface textures will be replicated onto the diamond surface during pressing. From the viewpoint of mold life, a molding temperature higher than 800 °C is not recommended in the present process.

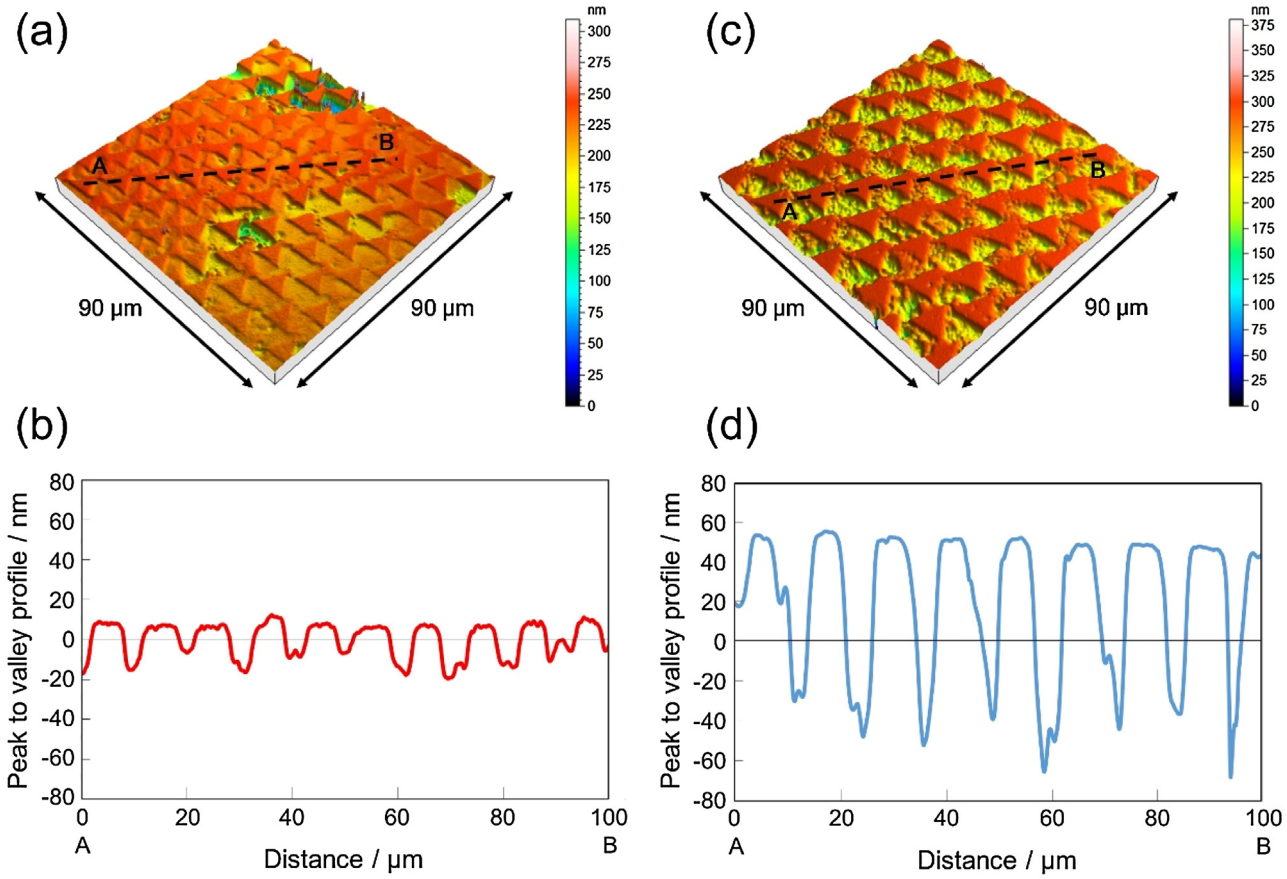

Fig. 11. Three- and two-dimensional surface profiles of diamond samples pressed under various pressures: (a) (b): 30 MPa, (c) (d): 60 MPa.

4.4. Effect of molding pressure

Molding pressure might be an important factor for controlling the thermochemical reaction. To investigate the effect of pressure, molding experiments under different pressures were conducted. Fig. 11 shows three- and two-dimensional surface profiles of diamond samples pressed under molding pressures of 30 MPa and 60 MPa. The two-dimensional profiles were obtained along the dotted lines indicated on the three-dimensional ones. The processing depth was measured from the two-dimensional profiles as the distance between the top surface (the non-reacted area) and the bottom surface (the reacted area) of the microstructures. The mean value of the processing depth was calculated from a total of 20 measurements. When the molding pressure was 30 MPa, the processing depth was 20 (±5) nm. The processing depth increased to 83 (±12) nm when the molding pressure was increased to 60 MPa. This result demonstrated that the thermochemical reaction between diamond and Ni was accelerated by pressure. When molding was conducted without pressure (0 MPa), however, no microstructures were confirmed on the diamond surface. In case of no pressure, the contact between the diamond sample and the Ni mold is incomplete, blocking the interfacial carbon diffusion. Therefore, it is important to use a sufficient pressure to imprint uniform microstructures on diamond. A high pressure improves thermochemical reaction speed and enables imprinting microstructures deeper and faster, and on an uneven diamond surface.

4.5. Effect of molding temperature

Temperature might be another important factor for the thermochemical imprinting process. For examining the effect of temperature, the diamond samples imprinted at 600 °C, 650 °C, 700 °C, 750 °C and 800 °C under the same pressure (30 MPa) were compared. The processing depth at each temperature was measured and plotted in Fig. 12. When temperature is below 650 °C, thermochemical reaction did not occur. The processing depth increases gradually in the range of 700–800 °C. It indicates that the thermochemical reaction is promoted at a higher temperature. Therefore, the depth of thermochemical imprinting can be controlled precisely by temperature and pressure.

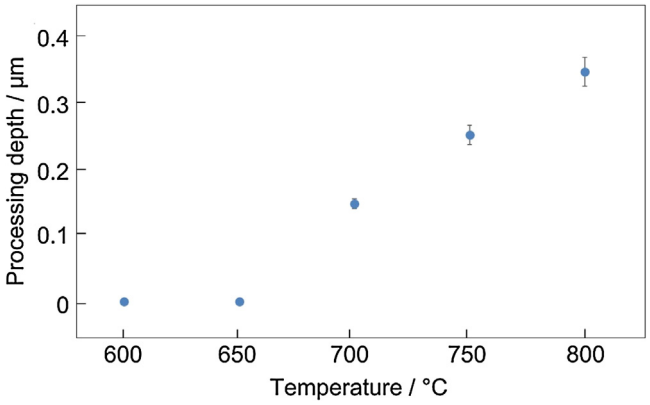

Fig. 12. Effect of temperature on processing depth of thermochemical imprinting.

In addition, it is known from the Ni-C phase diagram [26] that the amount of carbon diffusion to Ni is limited by temperature and pressure. The speed of the thermochemical reaction between Ni and diamond can be described by the Arrhenius equation [27]. Therefore, the diffusion of carbon will saturate at a point decided

by the temperature and pressure used. After the diffusion of carbon has saturated, the graphitization process stops, even if a longer heating and pressing time is set. The point of saturation will be investigated quantitatively as a future task in this study.

5. Conclusions

Thermochemical imprinting process of single-crystal diamond using a Ni mold under high temperature and pressure was investigated. The following conclusions were obtained:

(1) The shape of microstructures formed on the Ni mold using a nanoindenter system can be imprinted onto diamond surface through carbon diffusion-based thermochemical reaction.
(2) During thermochemical imprinting, a graphite layer will be formed on the diamond surface, which can be removed by washing with acid.
(3) Pressure has a strong effect on the thermochemical reaction. A higher pressure leads to a larger processing depth.
(4) The imprinting depth of microstructures increases with temperature. A temperature higher than 650 °C is necessary to activate the thermochemical reaction.
(5) At a high temperature (~800 °C), the Ni mold surface is roughened with rugged and tessellated textures after heating, and these textures are further transferred to the diamond surface during imprinting.

The present study has demonstrated the feasibility of a cost-efficient method to fabricate large-area microstructures on single-crystal diamond. This method is expected to be useful for creating micro surface patterns on diamond for cutting tools, optical elements, semiconductor substrates, and so on. One of the future tasks is to investigate the performance of other mold materials such as Fe, Ti, Co, etc., in the thermochemical imprinting process.

Acknowledgments

The authors would like to thank Asahi Diamond Industrial Co., Ltd. for providing single-crystal diamond samples, and Toshiba Machine Co., Ltd. for providing technical assistance in renovating the press molding machine used for the present experiments.

Reference:

[1] H. Al Mehedi, J.C. Arnault, D. Eon, C. Hébert, D. Carole, F. Omnes, E. Gheeraert, Etching mechanism of diamond by Ni nanoparticles for fabrication of nanopores, Carbon 59 (2013) 448–456.
[2] T. Yamada, H. Yoshikawa, H. Uetsuka, S. Kumaragurubaran, N. Tokuda, S. ichi Shikata, Cycle of two-step etching process using ICP for diamond MEMS applications, Diam. Relat. Mater. 16 (2007) 996–999.
[3] B.J.M. Hausmann, M. Khan, Y. Zhang, T.M. Babinec, K. Martinick, M. McCutcheon, P.R. Hemmer, M. Lončar, Fabrication of diamond nanowires for quantum information processing applications, Diam. Relat. Mater. 19 (2010) 621–629.
[4] D.P. Adams, M.J. Vasile, T.M. Mayer, V.C. Hodges, Focused ion beam milling of diamond: Effects of H[sub 2]O on yield, surface morphology and microstructure, J. Vac. Sci. Technol. B Microelectron. Nanometer Struct. 21 (2003) 2334.
[5] E. Paul, C.J. Evans, A. Mangamelli, M.L. Mcglauflin, R.S. Polvanit, Chemical aspects of tool wear in single point diamond turning, Precis. Eng. 18 (1996) 4–19.
[6] S. Shimada, H. Tanaka, M. Higuchi, T. Yamaguchi, O. Prefecture, D. Corp, Thermo-chemical wear mechanism of diamond tool in machining of ferrous metals, CIRP Ann. – Manuf. Technol. 53 (2004) 57–60.
[7] E. Brinksmeier, R. Glabe, J. Osmer, Ultra-precision diamond cutting of steel molds, CIRP Ann. – Manuf. Technol. 55 (2006) 551–554.
[8] T.F. Dai, F.Z. Fang, X.T. Hu, Tool wear study in diamond turning of steels, J. Vac. Sci. Technol. B Microelectron. Nanometer Struct. 27 (2009) 1335.
[9] L. Zou, G. Dong, M. Zhou, Investigation on frictional wear of Single-crystal diamond against ferrous metals, Int. J. Refract. Met. Hard Mater. 41 (2013) 174–179.
[10] W.J. Zong, T. Sun, D. Li, K. Cheng, Z.Q. Li, Nano-precision diamond cutting tools achieved by mechanical lapping versus thermo-mechanical lapping, Diam. Relat. Mater. 17 (2008).
[11] N. Furushiro, M. Higuchi, T. Yamaguchi, S. Shimada, K. Obata, Polishing of single point diamond tool based on thermo-chemical reaction with copper, Precis. Eng. 33 (2009) 486–491.
[12] H. Mehedi, C. Hebert, S. Ruffinatto, D. Eon, F. Omnes, E. Gheeraert, Formation of oriented nanostructures in diamond using metallic nanoparticles, Nanotechnology 23 (2012) 455302.
[13] L. Zhou, S.T. Huang, X.L. Wang, L.F. Xu, High-speed mechanical lapping of CVD diamond films using diamond wheel, Int. J. Refract. Met. Hard Mater. 35 (2012) 185–190.
[14] I. Shpilevaya, W. Smirnov, S. Hirsz, N. Yang, C.E. Nebel, J.S. Foord, Nanostructured diamond decorated with Pt particles: preparation and electrochemistry, RSC Adv. 4 (2014).
[15] W. Janssen, E. Gheeraert, Dry etching of diamond nanowires using self-organized metal droplet masks, Diam. Relat. Mater. 20 (2011) 389–394.
[16] J. Wang, L. Wan, J. Chen, J. Yan, Anisotropy of synthetic diamond in catalytic etching using iron powder, Appl. Surf. Sci. 346 (2015) 388–393.
[17] Y. Morofushi, H. Matsushita, N. Miki, Microscale patterning of Single-crystal diamond by thermochemical reaction between sidero-metal and diamond, Precis. Eng. 35 (2011) 490–495.
[18] J. Wang, L. Wan, J. Chen, J. Yan, Surface patterning of synthetic diamond crystallites using nickel powder, Diam. Relat. Mater. 66 (2016) 206–212.
[19] R. Narulkar, S. Bukkapatnam, L.M. Raff, R. Komanduri, Graphitization as a precursor to wear of diamond in machining pure iron: a molecular dynamics investigation, Comput. Mater. Sci. 45 (2009) 358–366.
[20] M. Uemura, An analysis of the catalysis of Fe, Ni or Co on the wear of diamonds, Tribol. Int. 37 (2004) 887–892.
[21] M. Yang, C.F. Yoshikawa, On polishing of diamond film with hot metal: the optimum polishing condition, J. Jpn. Soc. Precis. Eng. 57 (1991) 184–189.
[22] L.A.J. Garvie, A.J. Craven, R. Brydson, Use of electron-energy loss near-edge fine structure in the study of minerals, Am. Miner. 79 (1994) 411–425.
[23] V. Pichot, M. Comet, E. Fousson, C. Baras, A. Senger, F. Le Normand, D. Spitzer, An efficient purification method for detonation nanodiamonds, Diam. Relat. Mater. 17 (2008) 13–22.
[24] A.M. Schrand, L. Dai, J.J. Schlager, S.M. Hussain, E. Osawa, Differential biocompatibility of carbon nanotubes and nanodiamonds, Diam. Relat. Mater. 16 (2007) 2118–2123.
[25] D.S. Knight, W.B. White, Characterization of diamond films by Raman spectroscopy, J. Mater. Res. 4 (1989) 385–393.
[26] B.M. Singleton, P. Nash, The C-Ni (carbon-nickel) system, J. Phase Equilib. 10 (1989) 121–126.
[27] N. Furushiro, H. Tanaka, M. Higuchi, T. Yamaguchi, S. Shimada, Suppression mechanism of tool wear by phosphorous addition in diamond turning of electroless nickel deposits, CIRP Ann. – Manuf. Technol. 59 (2010) 105–108.